

Water Productivity Analysis: Irrigation Season 2019

APSAN-Vale project



REPORT

201

CLIENT

**Agência de desenvolvimento do
Vale Zambeze (ADVZ)**

AUTHORS

**Jonna van Opstal
Alexander Kaune
Martijn de Klerk**

DATE

March 2020

Water Productivity Analysis: Irrigation Season 2019

APSAN-Vale project

FutureWater Report 201

Client

Agência de desenvolvimento do Vale Zambeze (ADVZ)

Authors

Jonna van Opstal – Senior Water Productivity Expert (j.vanopstal@futurewater.nl)

Alexander Kaune – Agro-hydrologist (a.kaune@futurewater.nl)

Martijn de Klerk – Flying Sensor Expert, Project Manager (m.deklerk@futurewater.nl)

APSAN-Vale project partners

Resilience B.V.

HUB

Date

March 2020

FutureWater

ADDRESS

FutureWater B.V.
Costerweg 1V
6702 AA Wageningen
The Netherlands

TELEPHONE

+31 317 460 050

WEBSITE

www.futurewater.eu

Preface

The APSAN-Vale project has as its overall aim to increase climate resilient agricultural productivity and food security, with a specific objective to increase the water productivity and profitability of smallholder farmers in Mozambique, prioritizing small (family sector) farmers to increase food and nutritional security. This project will demonstrate what the best combinations are of adoption strategies and technological packages, with the largest overall impact in terms of Water Productivity, both at the plot-level, sub-basin as well as basin level. The main role of FutureWater is monitoring water productivity in target areas (both spatial and seasonal/annual variation) using remote sensing data from Flying Sensors (drones) and WaPOR in combination with a water productivity simulation model and field observations. This report shows the water productivity analysis for the irrigation season 2019 in three different locations in Mozambique. This analysis is crucial to evaluate the impact of field interventions on water productivity.

Summary

Farmers are seeking best practices that can achieve higher crop yields, thus profits and food security. With limited resources such as water, the increase of production needs to be considered per unit of water consumed, which is expressed in the term Water Productivity. Water productivity can be used as a performance indicator to monitor changes in an agricultural area (at plot, farm, or irrigation system level). If interventions are implemented, water productivity can indicate if the intervention had a positive or negative impact on the use of water or remained unchanged. This report provides an assessment of the water productivity during the irrigation growing season of 2019 (May to October) for the APSAN-Vale project areas.

At field scale a crop-specific water productivity is calculated using Flying Sensors and AquaCrop model simulations. Flying Sensors are equipped with a Near-Infrared camera for detection of the vegetation status. These images are processed and translate to canopy cover values. In AquaCrop the field data and canopy cover from flying sensors is used to simulate the farming practices for each field. At basin-scale the biomass water productivity is calculating using data from FAO's water productivity data portal WaPOR (<http://wapor.apps.fao.org>).

The crop-specific water productivity of tomato and cabbage of a location in Nhamatanda was on average 2.48 kg/m³ and 1.42 kg/m³ respectively. These values in comparison with the baseline values conveyed an increase in water productivity of 115% for tomato and 17% for cabbage. These are based on local practices implemented by the farmers.

An analysis at a larger scale is required to determine the overall water productivity increase and the impact of the project on the adoption of practices. At basin scale the biomass water productivity was 1.76, 1.75, and 1.43 kg/m³ for Bárúè, Moatize, and Nhamatanda respectively. In comparison with the baseline values the increase in water productivity was 17%, 18%, and 9% respectively. This is a positive trend and requires further investigation to determine to what magnitude the increase is related to the field interventions and adoption by the community.

Content

Summary	4
List of Tables	7
List of Figures	7
1 Introduction	8
1.1 Water productivity concept	8
1.2 APSAN-Vale project	8
1.2.1 Description	8
1.2.2 Logframe indicators	9
1.3 Season overview	10
1.4 Reading guide	10
2 Methodology	11
2.1 Project locations	11
2.1.1 Small commercial farmers (Pequenos Produtores Comercial, PPC's)	11
2.1.2 Sub-basins / local communities	11
2.1.3 Basins	11
2.2 Approach	12
2.2.1 Crop specific water productivity	13
2.2.2 Biomass water productivity	13
2.3 Flying Sensor Imagery	14
2.3.1 Flying sensor equipment	14
2.3.2 Imagery acquisition	14
2.3.3 Imagery processing	15
2.4 Crop simulation modelling	15
2.4.1 AquaCrop	15
2.4.2 Input data	16
2.4.3 Calibration process	18
2.5 WaPOR datasets	19
2.5.1 Actual Evapotranspiration	19
2.5.2 Biomass production	19
2.5.3 Supplemental layers	19
3 Seasonal weather results	20
3.1 Reference evapotranspiration	20
3.2 Precipitation	21
4 Field scale Water Productivity results	23
4.1 Flying sensor imagery	23
4.2 Water Productivity from AquaCrop	25
5 Sub-basin scale Water productivity results	26
6 Basin scale Water Productivity results	27
7 Seasonal Water Productivity assessment	28
7.1 Normalization for annual weather conditions	28

7.2	Water productivity assessment at field level	28
7.3	Water productivity assessment at basin scale	29
8	Concluding remarks	30
	Annex 1 – Overview of input data	31
	Annex 2 – Comparison weather data	32
	Annex 3 – Additional basin results	33

List of Tables

Table 1. Logframe indicators related to Water Productivity.	9
Table 2 Overview of flights and area during the Irrigation Season of 2019	15
Table 3. Calibrated parameters for selected crops in Báruè, Moatize and Nhamatanda.	17
Table 4. Soil texture in each site.	18
Table 5 Calibration results of AquaCrop simulations	25
Table 6 Biomass water productivity [kg/m ³] for cropland pixels in the flight areas of the project	26
Table 7 Overview of statistics of water productivity, evapotranspiration, and biomass production for the basins of selected project districts	27
Table 8 Comparison of tomato and cabbage water productivity (in kg/m ³) with baseline values	29
Table 9 Comparison of biomass water productivity (kg/m ³) for irrigation season at basin scale with baseline	29

List of Figures

Figure 1 Location districts of APSAN project activities	9
Figure 2 Impact of Cyclone Idai on Rio Metuchira (Nhamatanda)	10
Figure 3 Location of selected PPC's monitored with flying sensor flights during the Irrigation Season 2019.	11
Figure 4 Delineation of (sub-) basins and streamlines for the three districts	12
Figure 5 Workflow for calculation of crop specific water productivity analysis	13
Figure 6. Workflow for biomass water productivity analysis.	13
Figure 7 Photo of the Flying Sensor in action	14
Figure 8 Illustration explaining the response of near infrared (NIR) wavelength to vegetation status...	14
Figure 9. Field data and output simulations of the AquaCrop model.	16
Figure 10. Soil characteristic in Moatize.	18
Figure 11 Five day average reference evapotranspiration for 2019 from TAHMO stations (Báruè, Nhamatanda) and satellite data products (Moatize)	20
Figure 12 Comparison of 2019 monthly reference evapotranspiration with long-term average (2001-2018) with satellite weather data products.	21
Figure 13 Daily precipitation for 2019 from TAHMO stations (Báruè, Nhamatanda) and CHIRPS (Moatize).	21
Figure 14 Comparison of 2019 monthly precipitation with long-term average (2001-2018) with CHIRPS data.	22
Figure 15 Aerial image from flying sensor flights for a PPC field in Nhamatanda (Sr. Zacarias) with cabbage (couve) and tomato (tomate).	23
Figure 16 Vegetation status using Near-Infrared camera from flying sensor flights for a PPC in Nhamatanda (Sr. Zacarias) with green having high (alto) vegetation and red having low (baixo) vegetation	24
Figure 17 Canopy cover values for a PPC in Nhamatanda (Sr. Zacarias) indicating for each field the average canopy cover (in %) .	24
Figure 18 Water productivity, crop yield, and evapotranspiration results from AquaCrop for fields of PPC in Nhamatanda (Sr. Zacarias) with cabbage (green outline) and tomato (red outline)	25
Figure 19 Biomass water productivity from WaPOR for flight areas (indicated as red outline)	26
Figure 20 Seasonal biomass water productivity for cropland pixels using WaPOR data portal	27
Figure 21 Comparison of reference ET as measured at the TAHMO stations of Báruè, Moatize, and Nhamatanda, and the reference ET as calculated using satellite data products (GLDAS and CFSR)	32
Figure 22 Seasonal actual evapotranspiration for the irrigation season from WaPOR data portal	33
Figure 23 Biomass production for the irrigation season from the WaPOR data portal	34

1 Introduction

1.1 Water productivity concept

In order to meet the future needs of food and fiber production, developing and developed countries need to focus more on efficient and sustainable use of land and water (Bastiaanssen and Steduto, 2017)¹. Farmers have been able to gain profit by increasing agricultural production per unit of land. However, it is key to include the water consumption component in agricultural production. This would allow to improve agricultural production per unit of water consumed.

Water productivity consists of two components: production (either as crop yield or biomass) and water consumed. Water consumption occurs through evapotranspiration which is the sum of plant transpiration through the stomata in the leaves, and evaporation that occurs from the soil surface and intercepted water by the leaves (Squire, 2004)². Within this project the use of evapotranspiration (versus irrigation application) was selected, because it represents the component of the water balance that cannot be re-used by downstream users in a river basin context. Return flows from agricultural areas (through runoff or subsurface flow) are available for re-use in the downstream areas if the quality of the water is sufficient. As such, water productivity can be expressed as:

$$\text{Biomass water productivity [kg/m}^3\text{]} = \frac{\text{Biomass production [kg]}}{\text{Evapotranspiration [m}^3\text{]}}$$

$$\text{Crop specific water productivity [kg/m}^3\text{]} = \frac{\text{Crop harvestable yield [kg]}}{\text{Seasonal evapotranspiration [m}^3\text{]}}$$

Water productivity can be used as a performance indicator to monitor changes in an agricultural area (at plot, farm, or irrigation system level). If interventions are implemented, water productivity can indicate if the intervention had a positive or negative impact on the use of water or remained unchanged. In addition, spatial information on water productivity can indicate areas that have higher performance (early adopters) and whether practices are taken over by other farmers.

1.2 APSAN-Vale project

1.2.1 Description

The APSAN-Vale project commenced end of 2018 and is a 3.5 year project with the objective to: 'Pilot innovations to increase the Water Productivity and Food security for Climate Resilient smallholder agriculture in the Zambezi valley of Mozambique'. Water productivity is used as an indicator to quantify the impact of the innovations on smallholder agriculture. These innovations can be technical packages (interventions and trainings), and adoption of lessons-learned through farmer-to-farmer communication. Information on water productivity needs to incorporate both temporal and spatial aspects. The temporal changes in water productivity indicates if an intervention resulted in an increase of water productivity. The spatial patterns in water productivity indicates if the knowledge is being adopted in the region and increased the overall water productivity of the locality, and district. Project activities take place in three districts namely: Bárùè, Moatize, and Nhamatanda. Within each district, various localities are selected for piloting innovations. The location of the districts and current project activities are shown in Figure 1.

¹ Bastiaanssen, W. G. M. and Steduto, P.: The water productivity score (WPS) at global and regional level: Methodology and first results from remote sensing measurements of wheat, rice and maize, *Sci. Total Environ.*, 575, 595–611, doi:10.1016/j.scitotenv.2016.09.032, 2017.

² Squire, G. L.: *Water Productivity in Agriculture: Limits and Opportunities for Improvement*. Edited by J. W. Kijne, R. Barker, D. Molden. Wallingford, UK: CABI Publishing (2003), pp. 352, ISBN 0-85199-669-8, *Exp. Agric.*, 40(3), 395–395, doi:10.1017/S0014479704372054, 2004.

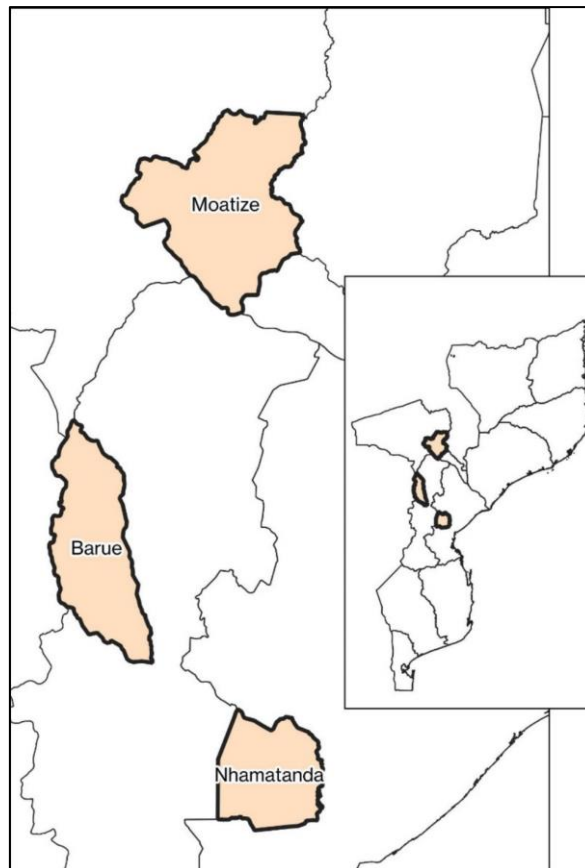


Figure 1 Location districts of APSAN project activities

1.2.2 Logframe indicators

Within the APSAN-Vale project several logframe indicators are formulated. The indicators linked with the water productivity assessment are listed in Table 1. Some indicators require the calculation of a crop specific water productivity (1.2 and 1.3), whilst other indicators use biomass water productivity (1.4). Also, the outputs indicate that water productivity is calculated at field, sub-basin, and basin scales, thus providing the required maps at those different spatial scales. The annual targets for the water productivity outcomes are percentages of increase compared to the baseline assessment (Van Opstal and Kaune, 2020)³ and are indicated in Table 1 as cumulative values, whereas the output maps are the annual total for each year.

Table 1. Logframe indicators related to Water Productivity.

	#	Indicator	Baseline	Target 2019	Target 2020	Target 2021
Goal	0.3	Increased Water Productivity	0%	7.5%	15%	25%
Outcome	1.2	Water footprint for selected crops	0%	7.5%	15%	25%
	1.3	Water productivity for maize	0%	7.5%	15%	25%
	1.4	Biomass water productivity	0%	7.5%	15%	25%
Outputs	1.1.1	# of field level maps	0	30	60	60
	1.1.2	# of sub-basin level maps	0	10	20	20
	1.1.3	# of basin level maps	0	6	12	12

³ Van Opstal, J.D., A. Kaune. 2020. Water Productivity Technical Report - Baseline assessment for APSAN-Vale project. FutureWater Report 195

1.3 Season overview

In March 2019 Cyclone Idai already caused major flooding in Moatize district and returned with catastrophic impact in Nhamatanda district. Figure 2 shows the areas of agricultural lands that vanished by the river Rio Metuchira, leaving heavy tolls on the local communities. Note that three out of the four demo plots in this area were washed away by the flooding. With urgency, land was being rehabilitated to be able to commence the irrigation growing season in a reasonable timing. Even with the efforts for quick land preparation, the planting of crops was delayed considerably compared to the baseline conditions.

For the three districts of the project location the flight area was changed. In the previous season a block of area within the same community and localidade (locality) was selected for monitoring with Flying Sensors. During this season it was decided to change the flight area in Nhamatanda and Bárue districts. Farmers that were selected to work with the project during this season were more widespread. Therefore, making flights of smaller blocks in different localidades, enabled monitoring of more farmers and thus covering more of the project activities on the ground.

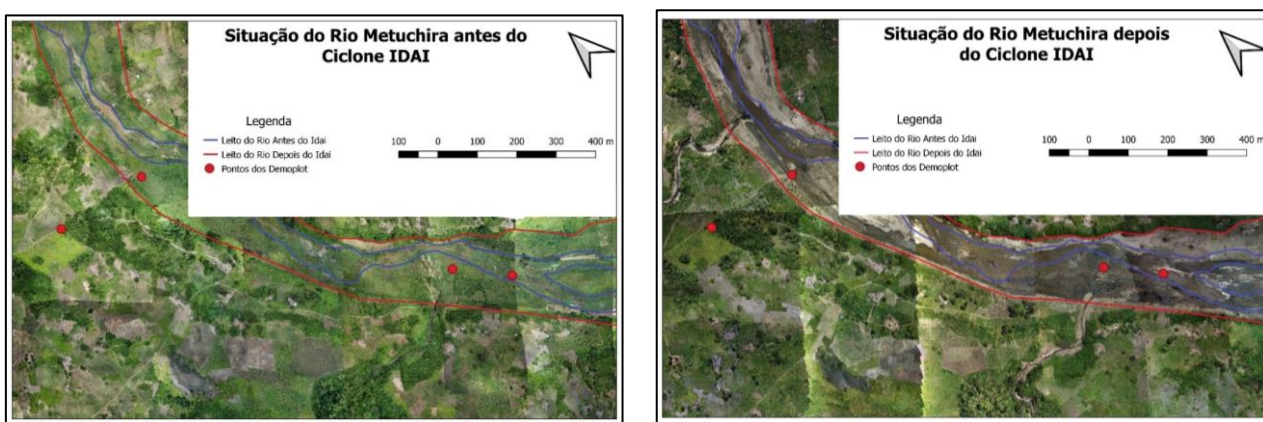


Figure 2 Impact of Cyclone Idai on Rio Metuchira (Nhamatanda)

1.4 Reading guide

This technical report provides the results of the water productivity analysis at field-scale and (sub-)basin scale using Flying Sensor Imagery, crop modelling, and FAO's WaPOR database. The next chapter (chapter 2) elaborates on the methodology used for conducting the water productivity analysis. Chapter 3 provides an analysis of the meteorological conditions during the growing season and compares with past years. Chapters 4, 5, and 6 provide the results of the water productivity analysis. Chapter 7 gives an assessment of the water productivity results and compares with the baseline assessment values. Chapter 8 provides the summarizing and concluding remarks.

2 Methodology

2.1 Project locations

2.1.1 Small commercial farmers (Pequenos Produtores Comercial, PPC's)

For each district several small commercial farmers (PPC's) were selected for the project to implement numerous innovative practices (boas praticas) for boosting water productivity. Most of the selected PPC's were monitored with flying sensor flights. For Moatize five PPC's were monitored all located in the vicinity of each other. For this reason, the flying sensor flights could be performed as one block. In contrast, for Bárue and Nhamatanda the PPC's were more widespread therefore flights were performed as multiple smaller blocks. In both Bárue and Nhamatanda five PPC's were monitored in each district. Figure 3 indicates the flight locations monitored during the irrigation growing season.

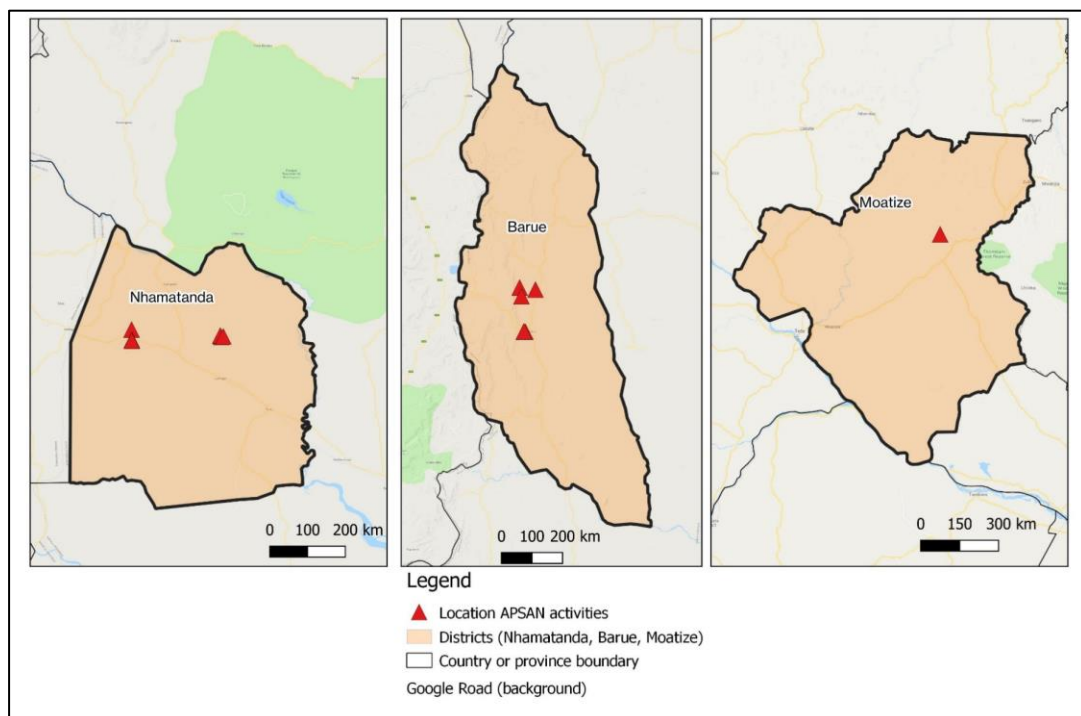


Figure 3 Location of selected PPC's monitored with flying sensor flights during the Irrigation Season 2019

2.1.2 Sub-basins / local communities

The sub-basin scale is a level between the field scale of the PPC's and the basin scale as described in the next section. For this report it is selected to select the sub-basin level at the size of local communities surrounding the PPC's. The objective of the APSAN-Vale project is to increase water productivity of several communities through knowledge exchange of the interventions being implemented. This is best monitored at a scale that captures the change of the communities. The area is selected using the flight area of the flying sensors, which encompass one or multiple PPC's and the surrounding farming community. The location of these communities are presented in figure 3, with three locations in Nhamatanda, four in Bárue, and one larger area in Moatize.

2.1.3 Basins

The basin delineation was performed using a DEM (digital elevation model) at 30m resolution provided by SRTM, and QGIS tools. Details on the steps involved can be reviewed in the manual (Kwast and

Menke, 2019)⁴. The outflow points for the sub-basins and basins are determined by evaluating the location of the project activities in the fields (as shown in Figure 3). The sub-basins should be representative for the streamflow that has influence on the localities of the project, whereas the basins represent the larger picture of the upstream area. The delineations and locations of project activities are shown in the maps of Figure 4. In Bárue, both a sub-basin and basin are delineated, where the sub-basin represents the upstream area of two (of the four) project locations. In Moatize, due to the size of the upstream area of the project location, only a basin is delineated. In Nhamatanda, two sub-basins are delineated and together form the basin. Measurements of water flow were conducted by project partners at strategic locations in the streams to quantify water abstractions for irrigation.

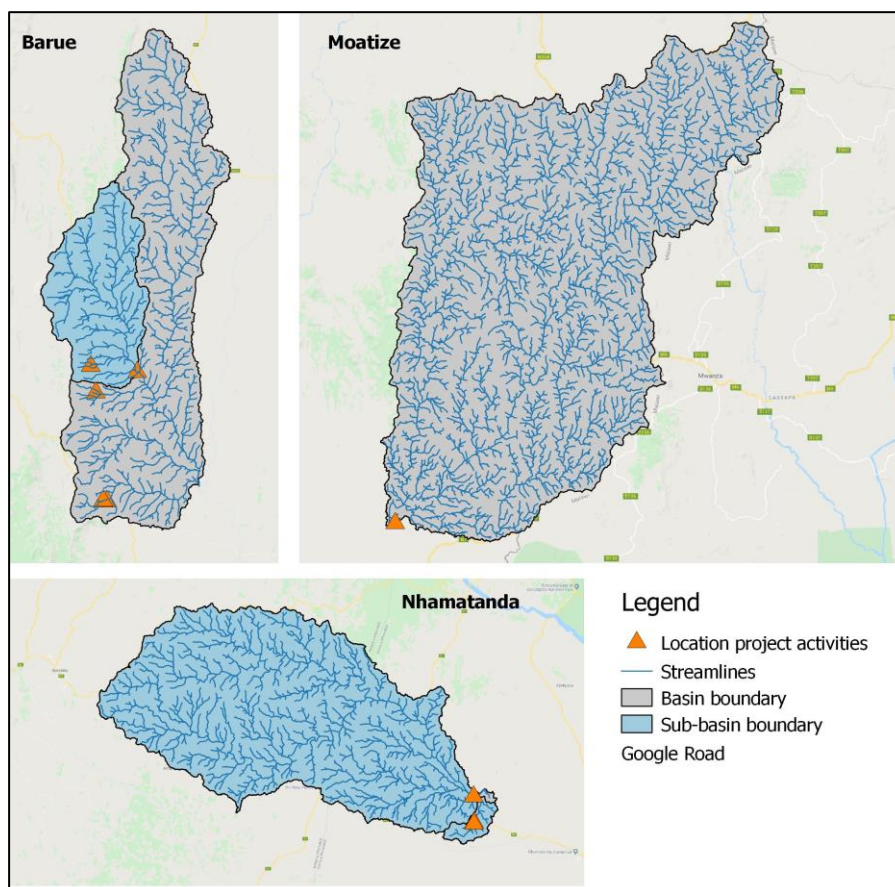


Figure 4 Delineation of (sub-) basins and streamlines for the three districts

2.2 Approach

The water productivity analysis follows two approaches for the calculation of water productivity:

1. At field scale the most detailed information is available regarding crop type and management strategies. At this scale a crop specific water productivity is calculated for the selected crops at the three different districts using crop simulation modelling (2.2.1).
2. At sub-basin and basin scale limited information is available on the spatial distribution of the crop types. At this scale a biomass water productivity is calculated using data from WaPOR, FAO's Open Access Portal with Water Productivity data (2.2.2).

⁴ van der Kwast, H. & Menke, K., QGIS for Hydrological Applications - Recipes for Catchment Hydrology and Water Management, Locate Press, 2019.

2.2.1 Crop specific water productivity

Figure 5 displays the workflow for performing the crop specific water productivity analysis. The water productivity is ultimately calculated with AquaCrop. Field data for setting up the AquaCrop simulations are taken from the weather station and field notebooks. Flying sensors capture images at regular intervals to calculate the canopy cover. This information is integrated with the AquaCrop model to calibrate the model and calculate water productivity. The advantage of combining remote sensing observations from flying sensors and simulation modelling, is that spatial insight is gained in the diversity of farm management practices. Thus, for each field the most fitting AquaCrop simulation run is selected to be representative for that field. In the next sections the various methods used are elaborated, namely the flying sensor imagery (2.3), and crop simulation modelling with AquaCrop (2.4).

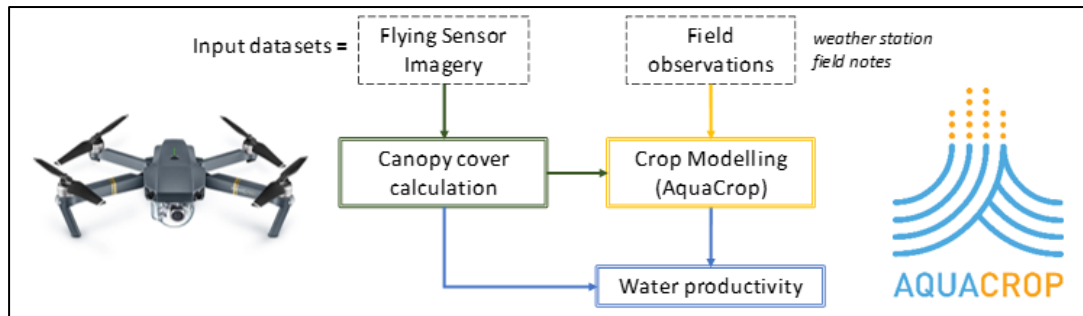


Figure 5 Workflow for calculation of crop specific water productivity analysis

2.2.2 Biomass water productivity

WaPOR is FAO's water productivity data portal containing information on evapotranspiration, biomass production, land cover, and many other layers. Information at basin scale was extracted by deriving a catchment delineation for the selected districts. This was performed using a DEM (digital elevation model). The catchment delineation is shown in figure 4 for the selected areas.

The land cover layer in WaPOR was used to determine the location of croplands in the basins. The procedure for this analysis follows the guidance provided by the WaterPIP project (Water Productivity in Practice) and the workflow is schematically presented in Figure 3. In section 2.5 the WaPOR datasets used for this analysis, is described with more detail.

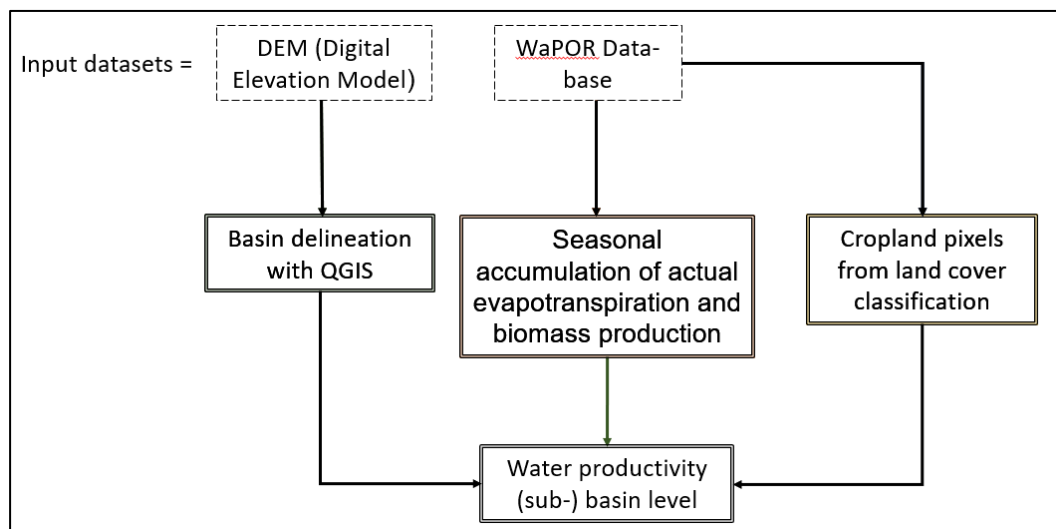


Figure 6. Workflow for biomass water productivity analysis

2.3 Flying Sensor Imagery

2.3.1 Flying sensor equipment

The Flying Sensor equipment used in APSAN-Vale are a Mavic Pro drone and an additional camera to detect vegetation status. Figure 7 shows a photo of the Flying Sensor used including both cameras. One camera makes RGB (red-green-blue) images, similar to visual images as seen with the human eye. The second camera measures the Near Infrared wavelength, which is not visible to the human eye. The near infrared (NIR) wavelength has a good response to the conditions of the vegetation. Figure 8 gives an illustration of the response to stressed conditions of a leaf. If the leaf is in optimal health the NIR wavelength has a high response. If the leaf is under stressed or sick conditions the NIR wavelength has a lower response. This is already measured by the NIR wavelength before it is visible to the human eye.



Figure 7 Photo of the Flying Sensor in action

Another advantage of using the Flying Sensors in this project is the flexibility for imagery capture and the high-spatial resolution of the acquired imagery. The flying sensors can make flights when required at the desired intervals. For this project the frequency of imagery acquisition was aimed at once every 3 weeks, which best captures the crop development stages. This interval was sometimes longer due to weather conditions or logistics. The spatial resolution of the imagery is 4-8 cm, providing sufficient detail to capture the spatial variation of small holder agriculture.

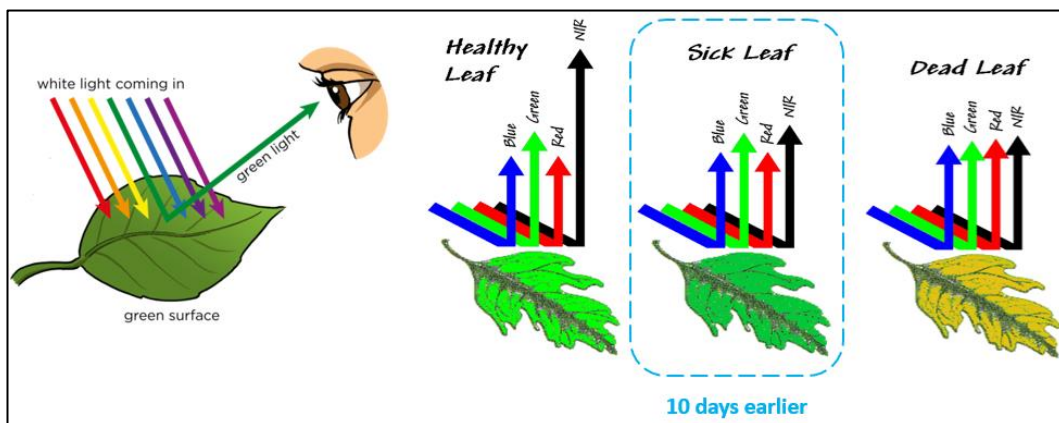


Figure 8 Illustration explaining the response of near infrared (NIR) wavelength to vegetation status

2.3.2 Imagery acquisition

Flying sensor images were acquired at regular intervals throughout the growing season. The flight area was changed during the growing season as indicated in section 1.3 due to adjustments in project activities. In table 2 an overview is provided of the number of flights performed and on which date (sometimes spread over 2 or 3 days). The total number of flights for Bárue, Nhamatanda, and Moatize, were 30, 40, and 41, respectively. The total area monitored with the flying sensors was 181 ha., 448 ha., and 446 ha. for Bárue, Nhamatanda, and Moatize respectively. A significant data gap exists in Moatize between the flight of early July and September.

Table 2 Overview of flights and area during the Irrigation Season of 2019

	Báruè	Nhamatanda	Moatize
Flight day(s) #1	5 flights, May 23rd	12 flights, May 21st	9 flights, May 15th
Flight day(s) #2	2 flights, June 27th	7 flights, July 3rd	10 flights, May 28th
Flight day(s) #3	3 flights, July 9th	7 flights, July 23rd	8 flights, May 29th
Flight day(s) #4	9 flights, July 25th	6 flights, August 8th	9 flights, July 7th
Flight day(s) #5	7 flights, August 19th	6 flights, August 27th	5 flights, Sep 4th
Flight day(s) #6	4 flights, Sep 12th	2 flight, Sep 17th	
Flights taken	30 flights total	40 flights total	41 flights total
Area covered	181 ha	448 ha	446 ha

2.3.3 Imagery processing

The imagery acquired by the Flying Sensors undergoes further processing. Firstly, the single images for each flight are stitched together to form an ortho mosaic. These are then georeferenced so it can be used in further geospatial analysis. These steps are performed using software packages: Agisoft Metashape, and QGIS (geospatial software). The resulting imagery is then further processed to create a raster image for each flight moment (1 or 2 days of single flights).

The next processing steps are required to achieve a time series of canopy cover maps. Several steps were calculated using R coding to make the processing more efficient. The NIR band of the image is used to determine the vegetation pixels of each image using the 'kmeans' R package for automatic imagery classification. Manually the user determines which class is appointed as vegetation. This information is then used to calculate the canopy cover, which is an indication of the vegetation cover over a surface in percentage and is in the same category as other vegetation indices commonly used in remote sensing e.g. Leaf Area Index (LAI) or Normalized Difference Vegetation Index (NDVI). Full vegetation cover will result in a canopy cover of 100%. A grid of 1x1 meter (=1 m²) is overlaid over a crop field. The number of vegetation pixels (of 0.05x0.05 meter = 0.0025 m²) is counted to determine the percentage of the grid that is covered by vegetation, thus the canopy cover. This information is used in combination with crop modelling to determine the crop yield, and water productivity.

2.4 Crop simulation modelling

2.4.1 AquaCrop

The AquaCrop model was selected for simulating the crop growth and water consumption, which is based on FAO principles as are reported in FAO Irrigation and Drainage Papers #56 and #66. It simulates both crop development and the water balance, resulting in crop water productivity results.

Several crop growth models have been developed to simulate crop yield and water productivity. The model selection depends on the application scale and the ability to constrain model parameter uncertainty. AquaCrop is a widely used crop model developed by FAO, which simulates the yield response to water using physically-based parameters. It has been used in climate change impact studies in various parts of the world (Hunink et al., 2014⁵; Hunink and Droogers, 2010⁶, 2011⁷). In addition, AquaCrop has been applied to predict water productivity and crop yield based on flying sensor

⁵ Hunink, J. E., Droogers, P. and Tran-mai, K.: Past and Future Trends in Crop Production and Food Demand and Supply in the Lower Mekong Basin., 2014.

⁶ Hunink, J. E. and Droogers, P.: Climate Change Impact Assessment on Crop Production in Albania. World Bank Study on Reducing Vulnerability to Climate Change in Europe and Central Asia (ECA) Agricultural Systems, FutureWater Report 105., 2010.

⁷ Hunink, J. E. and Droogers, P.: Climate Change Impact Assessment on Crop Production in Uzbekistan. World Bank Study on Reducing Vulnerability to Climate Change in Europe and Central Asia (ECA) Agricultural Systems, FutureWater Report 106., 2011

information (den Besten et al., 2017⁸, van Opstal, 2019⁹) and to assess irrigation scheduling scenarios (Goosheh et al., 2018¹⁰). It is specially recommended for small scale farm level application. In addition, it is an open source model which is freely available for application. Hence, the appropriate model for APSAN-Vale purposes.

FAO has preestablished model parameters to simulate the canopy cover, actual crop transpiration and soil evaporation, biomass and crop yield for a growth period from sowing to harvest (Figure 9). In this work, selected model parameters were tuned based on observations. Tuned model parameters included plant density, length of the growth period, increase in canopy cover, decrease in canopy cover, harvest index, fertility stress and cover of weeds.

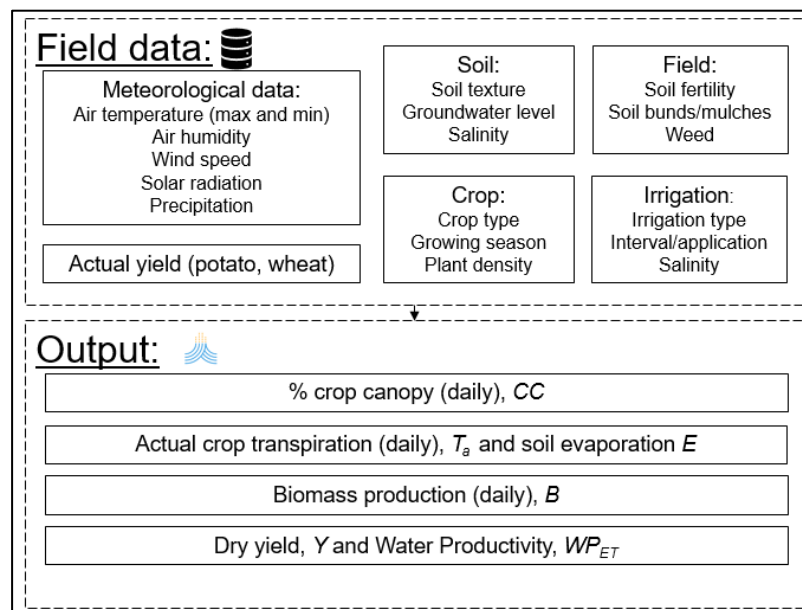


Figure 9. Field data and output simulations of the AquaCrop model.

2.4.2 Input data

Weather

Weather data is required as input for the model, which was derived from different sources. Weather stations (from TAHMO) were installed at each district office to represent the weather conditions in the area. These stations were operational from February / March 2019, which is halfway the rainfed season. Remote sensing data products were used to supplement the weather station data to fill in the gap at the start of the rainfed season. Precipitation and reference ET data were taken from WaPOR. Air temperature data was taken from GLDAS (Global Land Data Assimilation System)¹¹, which is a data product provided by NASA.

⁸ den Besten, N., Simons, G. and Hunink, J.: Water Productivity assessment using Flying Sensors and Crop Modelling. Pilot study for Maize in Mozambique, 2017.

⁹ Van Opstal, J.D.. 2019. APSAN-Vale Water Productivity Rainfed season 2018/2019. FutureWater Report.

¹⁰ Goosheh, M., Pazira, E., Gholami, A., Andarzian, B. and Panahpour, E.: Improving Irrigation Scheduling of Wheat to Increase Water Productivity in Shallow Groundwater Conditions Using Aquacrop, Irrig. Drain., 0(0), doi:10.1002/ird.2288, 2018.

¹¹ <https://ldas.gsfc.nasa.gov/gldas>

Field data

The next step is to collect basic crop information from the selected sites (Báruè, Moatize and Nhamatanda). Basic information about planting dates, plant density, total growth length (length of the crop cycle), and crop yield is key to obtain reliable AquaCrop simulations. Several of these parameters are specific for each field. Therefore, the notes taken in the fieldbook of the PPC's were copied to make the simulation tailored to the situation of the PPC. In Annex 1 the input data on management decisions can be found.

In the AquaCrop model several crop parameters must be used in order to simulate crop specific canopy cover, transpiration, biomass and yield during the growth season to finally determine the water productivity. Crop specific parameters were obtained from the original crop files available in the AquaCrop model. Crop files in Growing Degree Days mode ($^{\circ}\text{C}$ days) were used. The Growing Degree Days accounts for effects of temperature regimes on phenology. For Cabbage and Onion, we obtained the crop parameter information from other studies (Agbemabiese et al., 2017; Pawar et al., 2017; Pérez-Ortolá et al., 2015; Wellens et al., 2013).

Specific crop model parameters must be tuned to obtain accurate crop yields. In Table 3 the calibrated crop model parameters per crop are shown. These parameters include the Harvest Index, HI (%), Increase in Canopy Cover, CGC (-), Decrease in Canopy Cover, CDC (-), and the length of specific growing stages (e.g. sowing to emergence, sowing to maximum rooting depth, etc.). HI is a known parameter to convert biomass into crop yield. CGC is a measure of the intrinsic ability of the canopy to expand. After the canopy begins to senesce, the canopy cover is reduced progressively by applying an empirical canopy decline coefficient (CDC). HI, CGS and CDC vary depending on the crop variety and seed quality. The length of specific growing stages is used in Growing Degree Days mode ($^{\circ}\text{C}$ days) for Maize, Sorghum, Bean, Rice, Tomato, and Potato. For Cabbage and Onion, the calendar days mode is used based on the mentioned studies. The length of the growing stages was tuned based on the collected information of the length of the crop cycle (from planting to harvest in Table 3).

Table 3. Calibrated parameters for selected crops in Báruè, Moatize and Nhamatanda.

	Maize	Sorghum	Bean	Rice	Tomato	Potato	Cabbage*	Onion*
HI (%)	20	10	30	50	60	80	50	40
CGC (-)	0.0050	0.0048	0.0049	0.0084	0.0075	0.0162	0.1190	0.1190
CDC (-)	0.0040	0.0039	0.0044	0.0060	0.0040	0.0020	0.1000	0.1000
From sowing to emergence ($^{\circ}\text{C}$ days)	132	210	88	40	43	310	2	6
From sowing to maximum rooting depth ($^{\circ}\text{C}$ days)	2324	2453	1332	296	891	1672	40	77
From sowing to start senescence ($^{\circ}\text{C}$ days)	2310	2447	1354	1040	1553	1525	86	45
From sowing to maturity (length of crop cycle) ($^{\circ}\text{C}$ days)	2805	2728	1947	1520	1933	1977	100	85

From sowing to flowering (°C days)	1452	1613	834	920	525	852	28	67
Length of the flowering stage (°C days)	297	474	349	280	750	1	40	18

*Growing stages in calendar days.

Soil and field management information

According to collected field information the soil texture of each site was determined. The hydraulic properties of the soil are correlated with the soil texture. The AquaCrop model includes pre-established hydraulic properties such as Field Capacity (FC) and Wilting Point (WP) for each soil texture. Field Capacity and Wilting Point values are key to determine the soil water storage capacity and determine the water stress thresholds. In Table 44 the soil textures obtained for each site are shown. In Figure 1010, an example of FC and WP values (FC=22%, WP=10%) used in the AquaCrop model are shown for sandy loam.

Table 4. Soil texture in each site.

Site	Soil texture
Báruè	Clay
Moatize	Sandy Loam
Nhamatanda	Sandy Clay

```

1 deep uniform 'sandy loam' soil profile
2     6.0           : AquaCrop Version (March 2017)
3     46           : CN (Curve Number)
4     7           : Readily evaporable water from top layer (mm)
5     1           : number of soil horizons
6     -9          : variable no longer applicable
7     Thickness   Sat   FC   WP   Ksat   Penetrability   Gravel   CRa   CRb   description
8     --- (m) ---  --- (vol %) --- (mm/day) (%) (%) -----
9     4.00       41.0  22.0  10.0  1200.0   100           0       -0.323200  0.219363  sandy loam

```

Figure 10. Soil characteristic in Moatize.

2.4.3 Calibration process

The canopy cover follows a positive curvilinear trend throughout the growing season, representing the crop development until full cover. The flying sensors monitor the canopy cover throughout the growing season and thus capture at frequent intervals part of the curvilinear trend. This curvilinear trend is also simulated in AquaCrop. For the calibration process the canopy cover from the flying sensors is compared with the AquaCrop simulated canopy cover. This is done for the days that the flying sensors has acquired an image. In Table 2 it was noted that each district 5 to 6 flight moments occurred during the irrigation growing season. Thus, this provides 5 to 6 points of calibration with the AquaCrop model.

The AquaCrop model is set-up using the modules and input data as was listed in the previous sections. Then a number of parameters are selected that can be variable. These are particularly the variables that are sensitive in AquaCrop and cannot be accurately measured in the field. The parameters selected for calibration are: plant density, irrigation interval (days), irrigation depth, and fertilizer stress. After running the various combinations (244 simulation runs total per field) the top 10 to 15 simulations were selected displaying limited error with the canopy cover as observed from the flying sensor images.

2.5 WaPOR datasets

The FAO WaPOR database contains several datasets derived with satellite remote sensing and is available through the open access data portal: <https://wapor.apps.fao.org>. The layers used from WaPOR are: actual and reference evapotranspiration (ET), biomass production, water productivity, precipitation, and land cover. Detailed information on the methodology is found in the reference documents of WaPOR¹². The data layers were downloaded for Mozambique and aggregated to find seasonal values for the irrigation season: June 2019 to September 2019.

2.5.1 Actual Evapotranspiration

The actual evapotranspiration is calculated using a surface energy balance algorithm based on the equations of the ETLook model¹³. It uses a satellite platform with both multi-spectral and thermal imagery acquisition. In addition, meteorological data from remote sensing data products is used as input. The energy balance components are calculated with the specified algorithm: net radiation, soil heat flux, and sensible heat flux. The latent heat flux is calculated as residual to the energy balance and represents the evapotranspiration (ET) component of the energy balance.

The WaPOR actual ET dataset used in this report is from Level II (100 meter) for each decadal (10 days). A sum for the irrigation season is calculated in QGIS.

2.5.2 Biomass production

Biomass production was calculated using the decadal net primary production (NPP) data layer from WaPOR. The NPP data is calculated in WaPOR using a light use efficiency model¹⁴. This model determines the amount of photosynthetic radiation that arrives at a surface and the amount that is absorbed by vegetation depending on the amount of vegetational cover and (non-)stress conditions. This indicates the result of the photosynthesis process in NPP or dry matter biomass production. The biomass production from WaPOR is summed for the rainfed season. Note that WaPOR calculates biomass production for C3 crops, which are the majority of the crops grown globally. However, determining biomass production for C4 crops (e.g. maize, sugarcane) requires a multiplication of approximately 1.8 (=4.5/2.5) to correct for the difference in light use efficiency between the two crops. Crop yield can thereafter be calculated using the harvest index, which is specific for each crop type and crop variety (cultivar).

2.5.3 Supplemental layers

WaPOR also provides a precipitation data product, namely CHIRPS data. This provides spatial precipitation data at 5 km. resolution at daily time steps. This data is used supplemental to the weather station data to fill in data gaps where the weather station data was not installed.

In addition, reference evapotranspiration (ET) is also provided by the WaPOR data portal at 20 km. resolution and at daily time steps. A time series of this dataset is used as the required weather input data to the crop modelling.

Lastly, the land cover map in WaPOR is used to identify the pixels containing croplands. This is used to calculate the biomass water productivity for croplands, thus excluding the pixels of natural vegetation and urban areas.

¹² WaPOR Database Methodology: Level 1 data (September 2018) <http://www.fao.org/3/I7315EN/i7315en.pdf>

¹³ Bastiaanssen et al. (2012)

¹⁴ Hilker et al. (2008) and several other publications

3 Seasonal weather results

3.1 Reference evapotranspiration

At the TAHMO weather stations in each district, meteorological data is measured, and reference evapotranspiration is computed. The five day average reference evapotranspiration during the irrigation season is shown in Figure 11. The station located in Moatize displayed some data gaps during the season due to technical malfunctions. For this reason, weather data from satellite data products is displayed. In Annex 2 the comparison between TAHMO station data and the satellite data products is shown, indicating a good correlation between both datasets.

Figure 11 shows that reference evapotranspiration was lower at the start of the irrigation season and increased up to 5-7 mm/day at the end of the season. Moatize records higher reference evapotranspiration values, which is expected with the higher temperatures at this location.

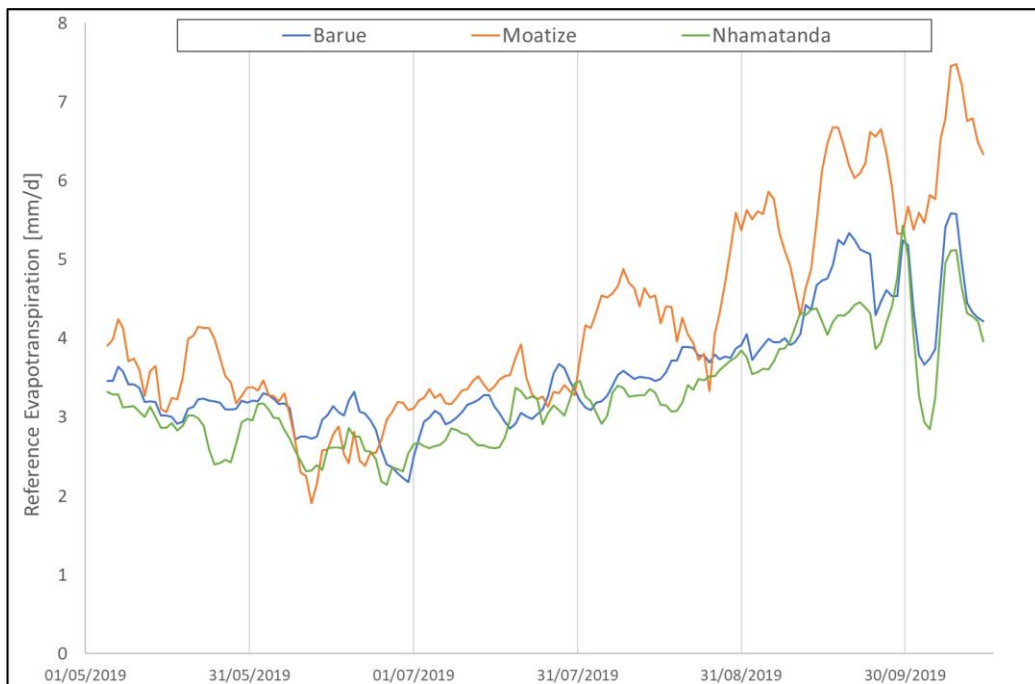


Figure 11 Five day average reference evapotranspiration for 2019 from TAHMO stations (Báruè, Nhamatanda) and satellite data products (Moatize)

The weather conditions during the 2019 irrigation season is compared with the historical dataset from 2001 to 2018, as used in the baseline assessment. This historical dataset covers a multitude of weather conditions, both dry and wet years, and therefore is a good representation of ‘normal’ weather conditions. The average monthly reference evapotranspiration is compared with the 2019 monthly values and displayed in Figure 12. All results are derived from the satellite data products, therefore avoiding dissimilarities due to different measuring methods. Figure 12 shows that for Nhamatanda and Báruè the reference evapotranspiration for this season was similar to the long-term average. Moatize displayed a slightly higher to reasonably higher reference evapotranspiration for each month.

Moatize in comparison with the other two districts, displays a higher or equal monthly reference evapotranspiration during the growing season. This can have impact on the crop modelling results which have weather data as input. Note, that water productivity is calculated with evapotranspiration in the denominator which is partly determined by the reference evapotranspiration during the season.

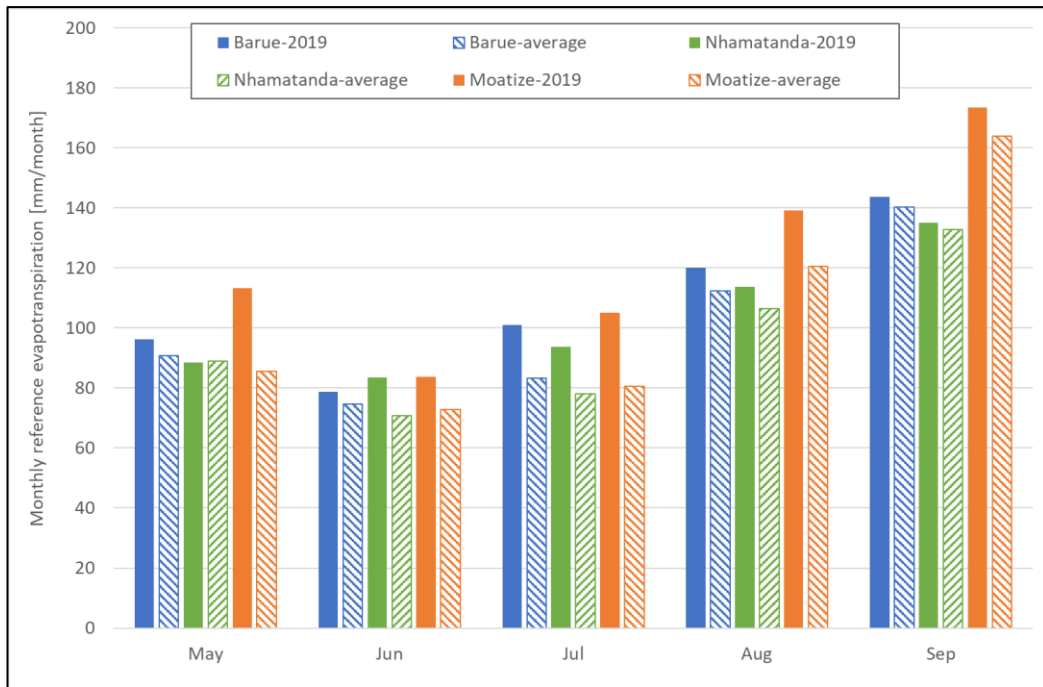


Figure 12 Comparison of 2019 monthly reference evapotranspiration with long-term average (2001-2018) with satellite weather data products

3.2 Precipitation

The irrigation season is also referred to as the dry season with less precipitation occurring during the season. The rainfall as recorded at the TAHMO stations (for Bárue and Nhamatanda) and satellite data (for Moatize) are presented in Figures 13 and 14. Figure 13 displays the daily precipitation and indicates several rainfall events occurred during the growing season. Rainfall events were more frequent in Nhamatanda than the other two districts.

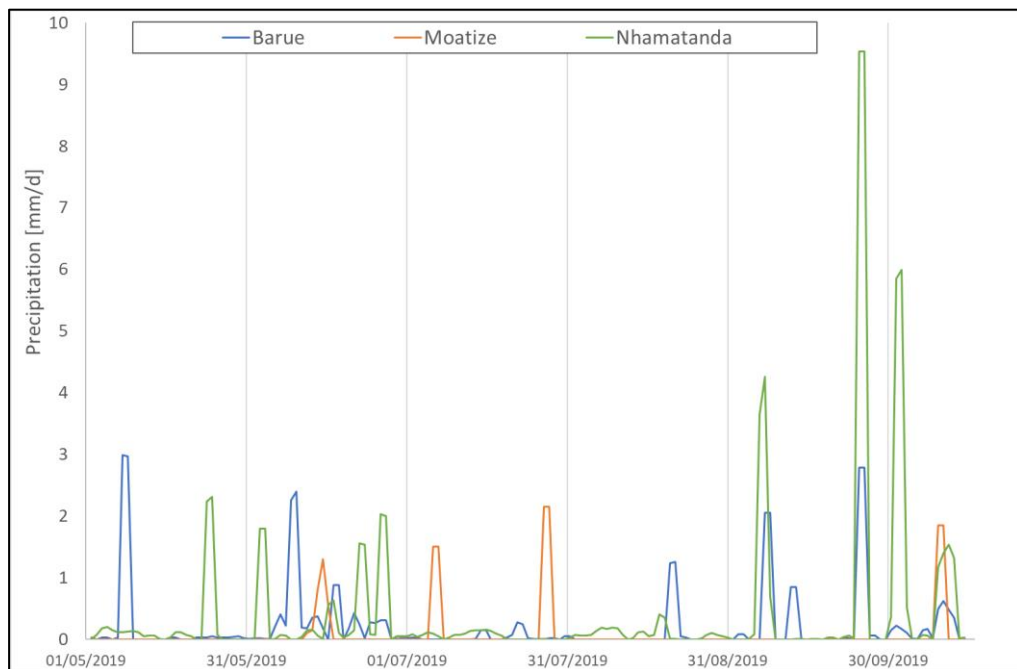


Figure 13 Daily precipitation for 2019 from TAHMO stations (Bárue, Nhamatanda) and CHIRPS (Moatize)

Figure 14 displays the monthly and seasonal total precipitation for each district and compares with the long-term average (2001-2018) using satellite data. The figure graph shows that the first three months the precipitation was generally below the long-term average. The seasonal total precipitation was well below the long-term average for all districts, particularly for Moatize being less than half of its average precipitation. During the irrigation growing season several farmers depend on irrigation water for the supply of water to their fields, and not solely precipitation. However, the decrease in precipitation can have influence on the total water supply in the basin and the water levels in the rivers that feed irrigation systems.

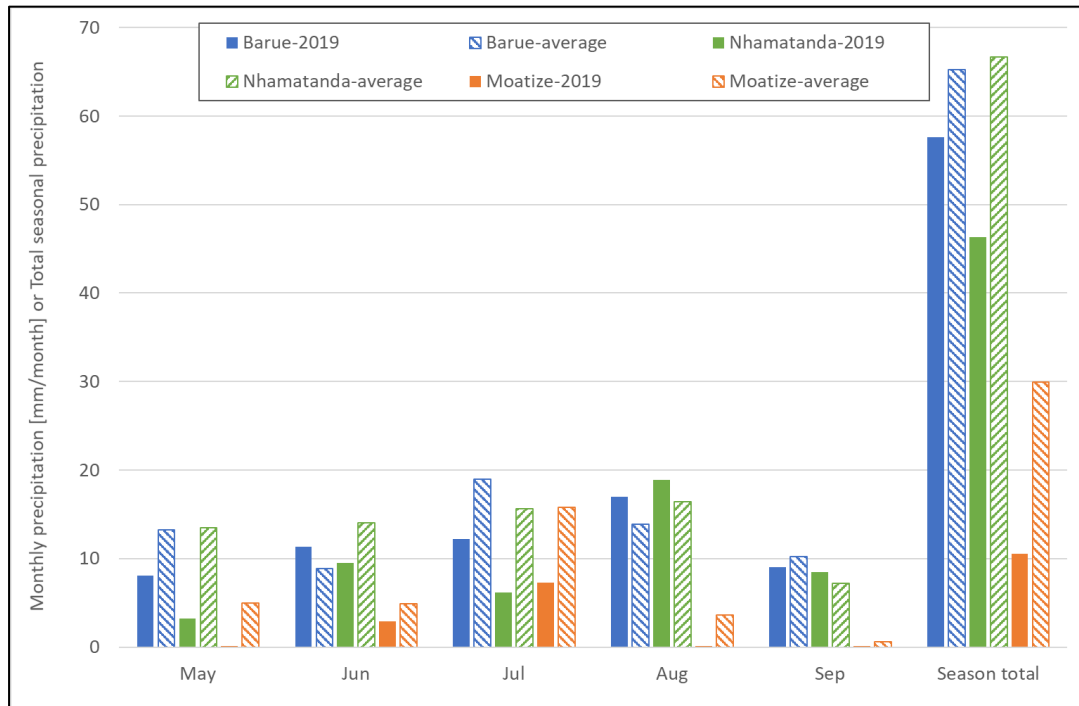


Figure 14 Comparison of 2019 monthly precipitation with long-term average (2001-2018) with CHIRPS data

4 Field scale Water Productivity results

4.1 Flying sensor imagery

Flying sensor images were acquired throughout the irrigation growing season. In Figure 15 an overview is provided of the aerial (RGB) images acquired at 5 flight dates for a PPC field in Nhamatanda. Two types of crops were grown on this field namely tomato and cabbage. From this image it can be perceived that the Southern tomato field was planted later, thus achieving full vegetation cover at a later stage than the other tomato field.

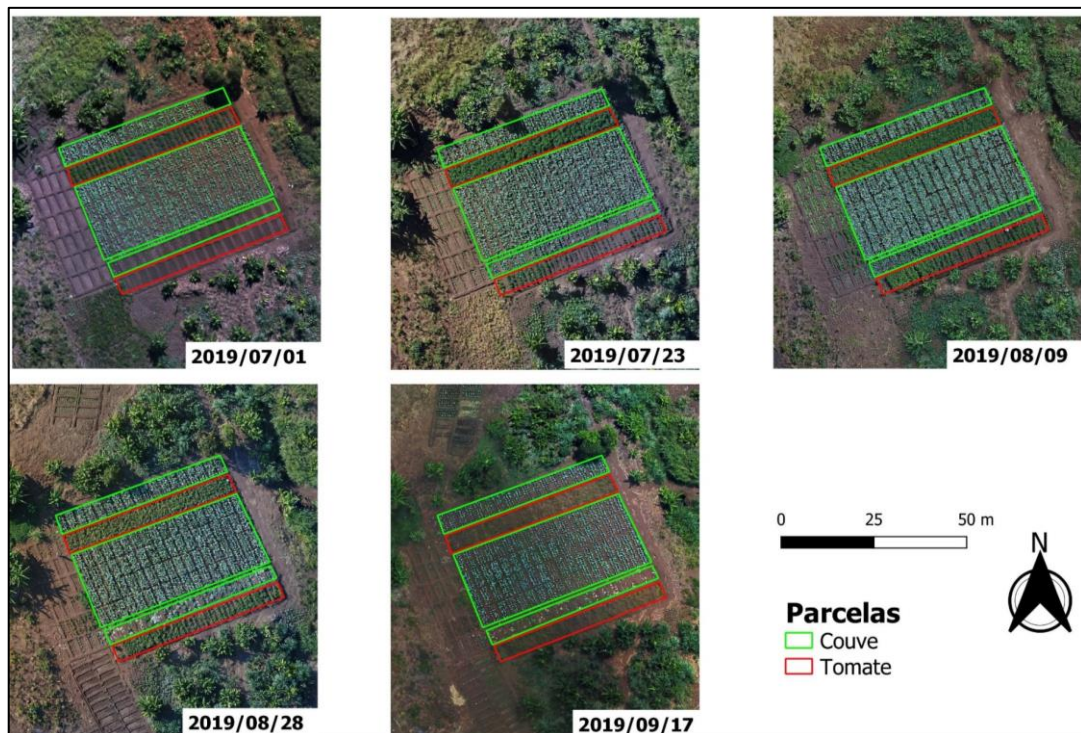


Figure 15 Aerial image from flying sensor flights for a PPC field in Nhamatanda (Sr. Zacarias) with cabbage (couve) and tomato (tomate)

Figure 16 displays an overview of the vegetation status images acquired at the same flight dates using the Near-Infrared camera. The maps show more detail in variation of vegetation cover within and between fields in comparison with the RGB images. This demonstrates the advantage of using a Near-Infrared camera, which is more sensitive to vegetation. Each field is typically divided in blocks separated by bunds and prevents irrigation losses by surface runoff. For the middle cabbage field, it is clearly displayed that some blocks have higher vegetation than others, perhaps due to the direction the irrigation water is applied.

For the calculation of canopy cover, the Near-Infrared band is used and classified for vegetation and non-vegetation pixels. The resulting canopy cover is shown in Figure 17 including the average canopy for each field. This information is used in the calibration of the AquaCrop modelling.

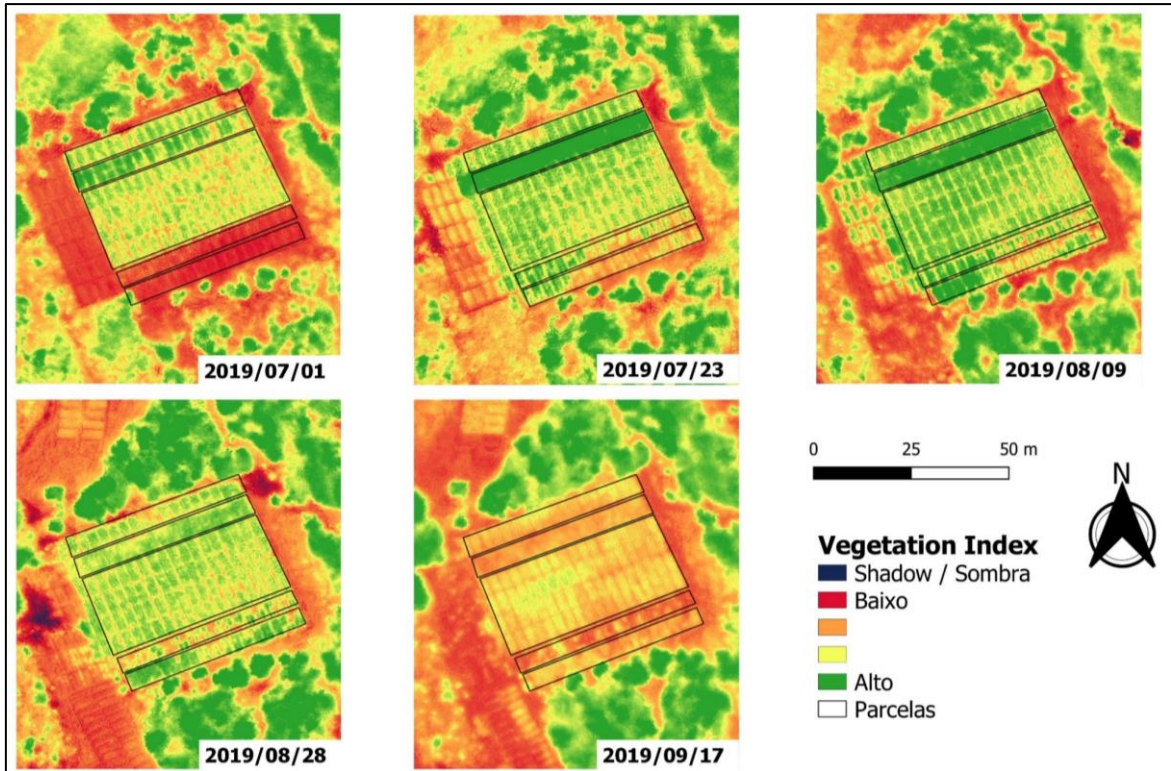


Figure 16 Vegetation status using Near-Infrared camera from flying sensor flights for a PPC in Nhamatanda (Sr. Zacarias) with green having high (alto) vegetation and red having low (baixo) vegetation

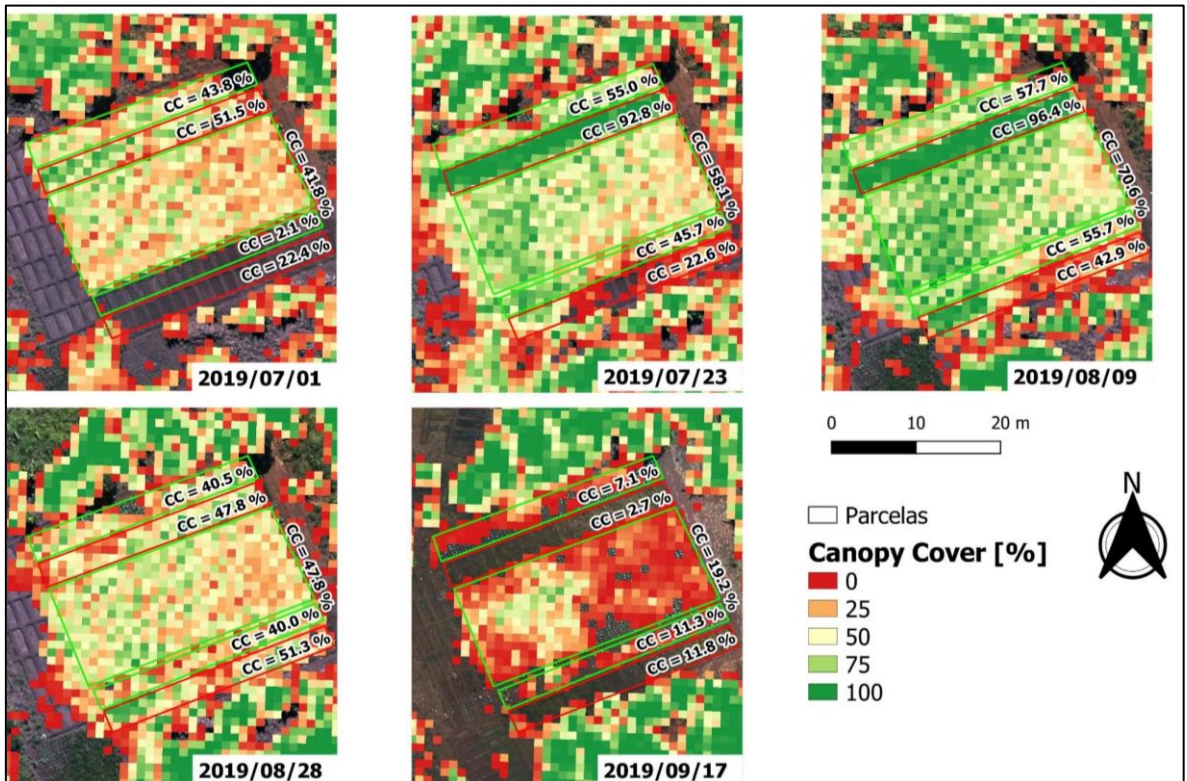


Figure 17 Canopy cover values for a PPC in Nhamatanda (Sr. Zacarias) indicating for each field the average canopy cover (in %)

4.2 Water Productivity from AquaCrop

The canopy cover as shown in Figure 17 was used to calibrate the AquaCrop model results. The simulations runs with the least amount of error were deemed the best fit for the field conditions and are used for determining the water productivity. Table 5 reports on the error that was found during the calibration process. The error in canopy cover gives information on the difference in canopy cover between the flying sensor image and the AquaCrop results. This value is a sum of all errors, namely for 5 to 6 flight moments. The coefficient of variation provides better insight in the magnitude of error by comparing the error in canopy of cover with the sum of all canopy covers. From Table 5 the Cabbage field (NH_ZF_01_03) displayed the leas error. This field is also the largest in size, which could have an impact on the result. Both the last two fields displayed the largest error. These were also planted at a later date, and perhaps the crop cycle could not be completed therefore discrepancies occurred.

Table 5 Calibration results of AquaCrop simulations

ID plot	Crop	Error in Canopy Cover %	Error expressed as Coefficient of Variation
NH_ZF_01_01	Cabbage	51.0	0.26
NH_ZF_01_02	Tomato	63.0	0.22
NH_ZF_01_03	Cabbage	31.8	0.15
NH_ZF_01_04	Cabbage	45.4	0.32
NH_ZF_01_05	Tomato	44.4	0.32

Figure 18 shows the assessment of water productivity, crop yield, and evapotranspiration resulting from the best-fit AquaCrop simulations. The water productivity of the tomato fields is highest with the tomato field that was planted first (on the North) showing a higher water productivity than the Southern tomato field. The cabbage fields display similar water productivity values and crop yield values. For evapotranspiration the tomato fields have larger quantities than the cabbage fields.

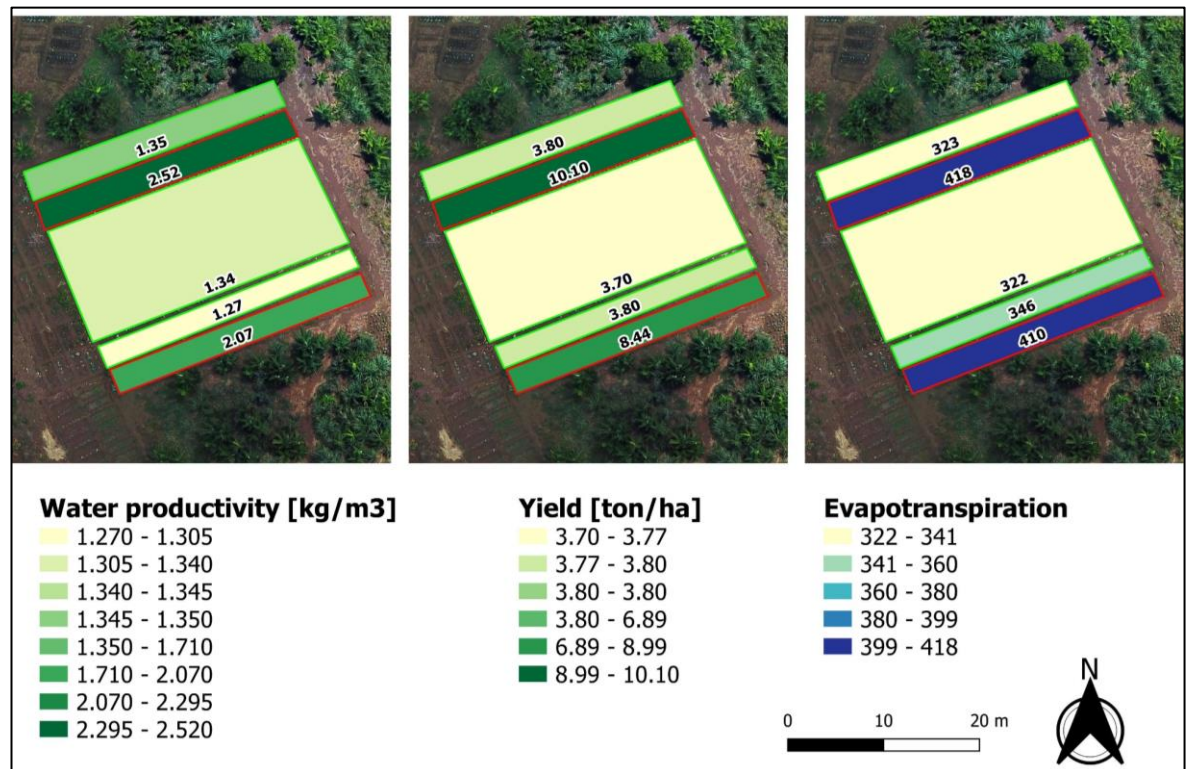


Figure 18 Water productivity, crop yield, and evapotranspiration results from AquaCrop for fields of PPC in Nhamatanda (Sr. Zacarias) with cabbage (green outline) and tomato (red outline)

5 Sub-basin scale Water productivity results

The sub-basin scale is determined to encompass the selected PPC and surrounding farming community based on the flight area locations. The WaPOR data portal provides the biomass water productivity and a classification of cropland pixels.

The results of the WaPOR assessment is shown in Table 6 indicating the average for each district. Figure 19 displays the location of the flights, which were used to determine the water productivity values. Moatize consisted of one location, Nhamatanda of 3 locations, and Bárue of 4 locations. The biomass water productivity was highest in Bárue, followed by Nhamatanda, and lastly Moatize.

Table 6 Biomass water productivity [kg/m³] for cropland pixels in the flight areas of the project

District	Sub-basin	Biomass water productivity [kg/m ³]	Average [kg/m ³]
Nhamatanda	I	1.31	1.30
	II	1.31	
	III	1.28	
Moatize	I	1.12	1.12
Bárue	I	1.55	1.65
	II	1.68	
	III	1.80	
	IV	1.57	

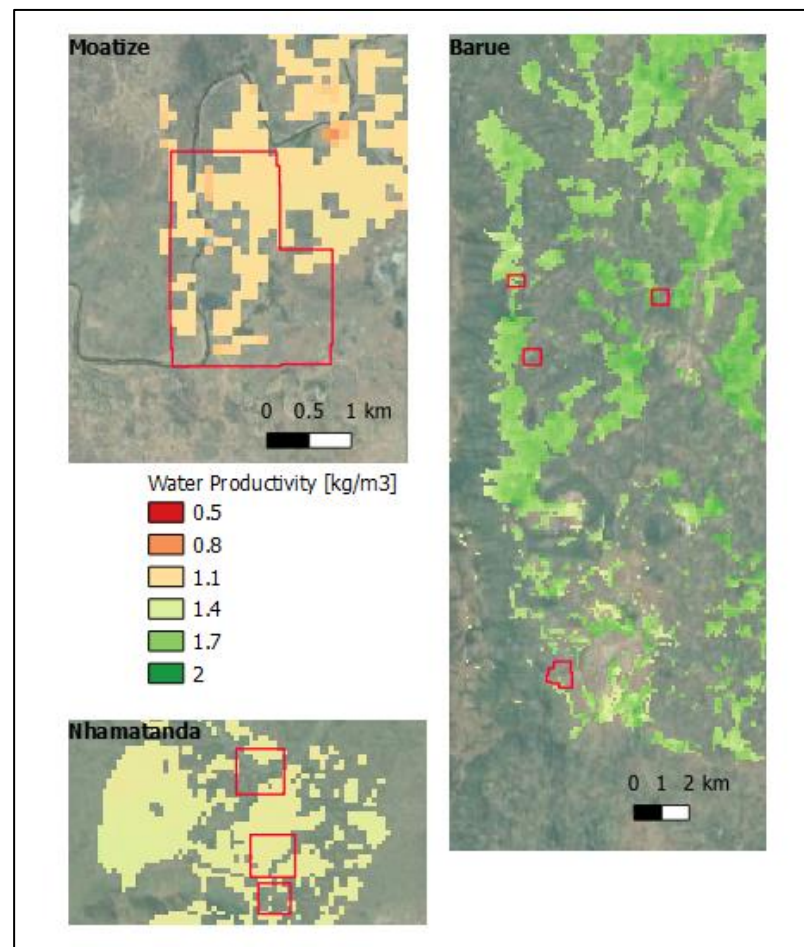


Figure 19 Biomass water productivity from WaPOR for flight areas (indicated as red outline)

6 Basin scale Water Productivity results

The basins were delineated for each district as shown in Figure 4. These delineations were used with the WaPOR data portal to determine the biomass water productivity for each location. Table 7 provides an overview of the statistics found for water productivity, evapotranspiration, and biomass production for each basin. The water productivity was highest for Báruè, followed by Moatize, and lastly Nhamatanda. The lower water productivity can be attributed to the higher values of evapotranspiration reported in WaPOR during the growing season. Báruè displays the highest biomass production of the area. Figure 20 displays the water productivity maps of each basin. In Báruè, the water productivity shows even distribution. In Moatize the upstream area displays higher water productivity values than downstream. These areas are also closer to the mountain range, which could influence the local weather conditions.

Table 7 Overview of statistics of water productivity, evapotranspiration, and biomass production for the basins of selected project districts

		Báruè	Moatize	Nhamatanda
Actual evapo- transpiration [mm]	Average mean	373	376	411
	10th percentile	288	304	339
	90th percentile	464	453	492
Biomass production [ton/ha]	Average mean	6.09	5.56	5.46
	10th percentile	4.79	4.55	4.49
	90th percentile	7.33	6.64	6.51
Water productivity [kg/m ³]	Average mean	1.64	1.49	1.33
	10th percentile	1.50	1.31	1.28
	90th percentile	1.77	1.68	1.40

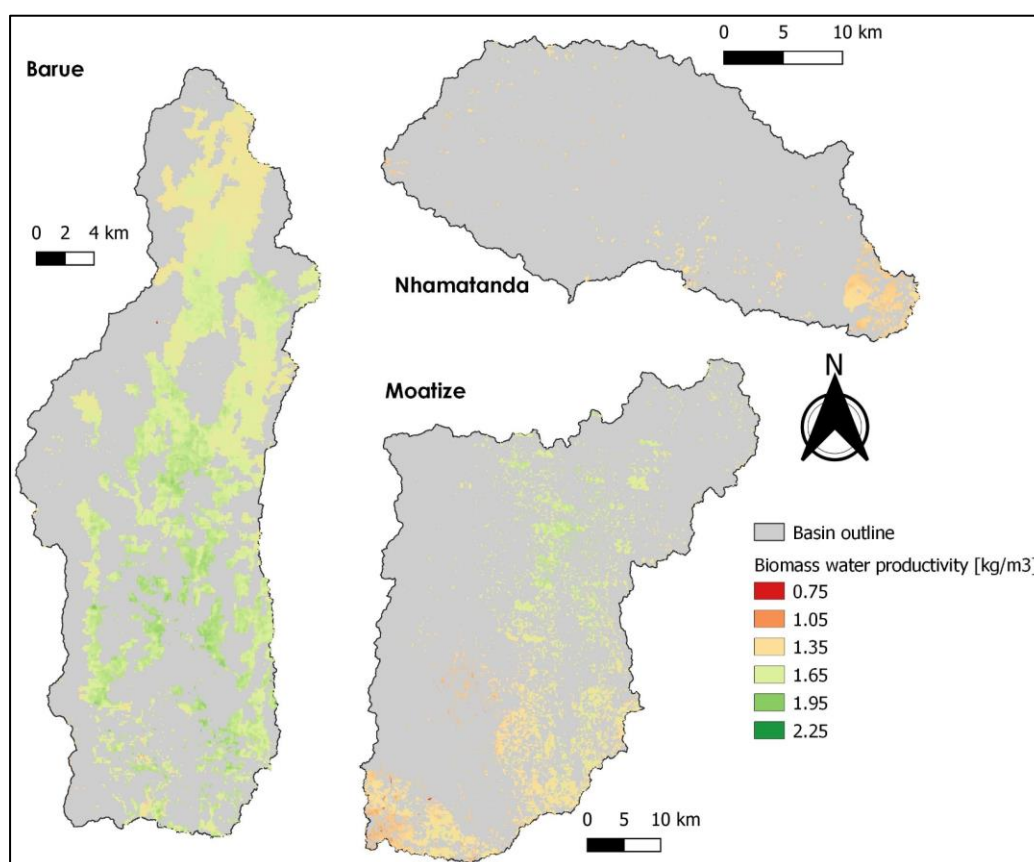


Figure 20 Seasonal biomass water productivity for cropland pixels using WaPOR data portal

7 Seasonal Water Productivity assessment

The baseline assessment water productivity report¹⁵ provided the average water productivity during an 17 year period (2001 – 2017). This is considered to be the baseline of the water productivity for the project locations, without any interventions placed by APSAN-Vale activities. During the irrigation season the project worked with several PPC's to improve the water productivity of their farm and subsequently also various PPE's (smallholder farmers) and surrounding communities.

Assessment of the water productivity is performed at two levels. Firstly, the change of water productivity due to specific interventions at the field of the PPC's is assessed. This level is considered the local scale of changing water productivity. Secondly, the change of water productivity of the surrounding communities is assessed. This will be influenced by neighboring PPE's and communities adopting the interventions. This level is considered the increase of the overall water productivity of the region.

During this season the activities were focused on a selection of PPC's and a number of communities. The following two sections elaborates on the change in water productivity of the PPC in comparison with the baseline report; and the change in overall water productivity using the WaPOR database to assess for a larger area. Both assessments make use of normalizing the water productivity for the seasonal weather conditions. Thus, changes in water productivity linked to the seasonal weather is reduced in the assessment. The method of normalization of the weather conditions is firstly explained, followed by the water productivity assessment at the level of the PPC, and lastly the overall water productivity assessment at the level of the (sub-)basin.

7.1 Normalization for annual weather conditions

For the baseline assessment a period of 17 years was used for the field scale analysis (2001 – 2017) and 10 years for the basin scale analysis (2009 – 2018). The period for the basin scale analysis was shorter due to the data availability of WaPOR. Both periods are deemed sufficient for capturing the inter-annual variability in weather conditions with both dry and wet years existing within a time frame of 10 years. The statistical results from this baseline analysis will therefore be representative for the variety of weather conditions.

In further analysis of this project, water productivity values will need to be normalized for weather conditions to determine if changes in water productivity are a result of weather conditions or the impact of the project innovations. The normalization of water productivity values is calculated by using the equation below (as example using the year 2019) and using reference evapotranspiration (ET_0) as representative for the annual weather conditions.

$$WP_{norm,2019} [kg/m^3] = \frac{WP_{2019} \left[\frac{kg}{m^3} \right] \times ET_{0,2019} [mm]}{ET_{0, average\ 2000-2019} [mm]}$$

7.2 Water productivity assessment at field level

Chapter 4 of this report presents the results of the field scale water productivity values. The field of a PPC in Nhamatanda is presented with water productivity values of tomato and cabbage, in Figure 18. The water productivity for tomato ranges from 2.07 – 2.52 kg/m³ and for cabbage from 1.27 – 1.35 kg/m³. After normalizing for weather conditions, the water productivity results are for tomato 2.23 – 2.72 kg/m³ and for cabbage 1.37 – 1.45 kg/m³. These values are reported in Table 8 and compared with the values from the baseline assessment report. The assessment shows that an increase of 95% was calculated for tomato and 4% increase for cabbage. For tomato a large increase was observed due to the

¹⁵ Van Opstal, J.D., A. Kaune. 2020. Water Productivity Technical Report - Baseline assessment for APSAN-Vale project. FutureWater Report 195.

implemented interventions. However, this is a one case example and is not representative for the overall water productivity increase achieved at other locations or the region as a whole.

Table 8 Comparison of tomato and cabbage water productivity (in kg/m³) with baseline values

	Tomato	Cabbage	Average
Baseline			
Range	1.02 – 1.35	0.781 – 1.549	
75 th Percentile	1.265	1.370	
Irrigation Season 2019			
Range	2.23 – 2.72	1.37 – 1.45	
Average (mean)	2.47	1.42	
Relative change (%)	+95%	+4%	+50%

7.3 Water productivity assessment at basin scale

The assessment of water productivity at basin scale was performed using the WaPOR results from chapter 5. These indicate the water productivity values for cropland pixels at the selected basins of the project for the irrigation season. Table 9 presents the values of biomass water productivity after normalizing for the 2019 weather conditions and comparing with the baseline values. An increase of biomass water productivity was perceived for all selected basins ranging from 9% to 18%. This is a positive trend and requires further investigation to determine to what magnitude the increase is related to the field interventions and adoption by the community.

Table 9 Comparison of biomass water productivity (kg/m³) for irrigation season at basin scale with baseline

	Báruè	Moatize	Nhamatanda	Average
Irrigation season 2019	1.64	1.49	1.33	
Irrigation season 2019 Normalized	1.76	1.75	1.43	
Baseline	1.50	1.48	1.31	
Relative change (%)	+17%	+18%	+9%	+15%

8 Concluding remarks

The water productivity results as presented in this report provide insight of the impact of the project activities both at field and basin level. Various methods were used to provide a reliable assessment of the water productivity, using the data available from the field.

The increase perceived at both the field and basin scale water productivity as presented in chapter 6 indicate a positive impact of the project in these regions. The expectation is that, following the expansion of project activities at field scale during the upcoming growing season, the overall water productivity will increase consequently, assuming that this positive trend will remain. Further investigation is required to determine the level of adoption of the interventions by the farming communities and the link with the observations as reported with the WaPOR analysis.

At field scale, the impact of individual interventions can be examined with further detail. In most fields, various interventions are practiced simultaneously. This project is a pilot project, therefore the upcoming seasons focus will also be made in the water productivity assessment to determine the level of impact each intervention has on the water productivity.

Lastly, the field scale analysis of the crop-specific water productivity as presented in this report was limited to a PPC in Nhamatanda. During the season changes were made in the selection of PPC and collection of field data and flight planning. This limited the analysis and provided insufficient data to draw accurate conclusions. For this reason, the analysis was replaced by using WaPOR data also at field scale. Despite the inaccuracies due to the limited spatial resolution of WaPOR, this dataset was deemed objective and sufficient for a general analysis also at field scale. In the upcoming growing season, the analysis will include several PPC's in the assessment of field scale crop-specific water productivity.

Annex 1 – Overview of input data

This table provides an overview of the data collected by local observations, information from local extensionist, past reports, and other data sources. Based on this information the AquaCrop runs were set-up.

ID plot	Soil		Crop				Field mgt				Irrigation			Yield	
	Soil texture (sandy/loam, etc)	Stoniness (low, moderate, high)	Crop type (EN)	Crop type (PT)	Planting date	Planting density [plants/m ²]	Fertilizer use (low, moderate, optimal)	Mulching yes/no	Weed mgt (low, moderate, high)	Runoff mgt (yes/no)	Irrigation (yes/no)	Irrigation method	Irrigation interval (days)	Irrigation depth (m ³ /ha)	Crop yield end of this season [ton/ha]
NH_ZF_01_01	sandy clay	moderate	Cabbage	Couve	01/Jun	2.5	Optimal	no	Low	yes	yes	bacia	2 dias	Bomba pedestral 44 L/m	18.0
NH_ZF_01_02	sandy clay	moderate	Tomato	Tomate	01/Jun	2.6	Optimal	no	Low	yes	yes	bacia	2 dias	Bomba pedestral 44 L/m	12.0
NH_ZF_01_03	sandy clay	moderate	Cabbage	Couve	01/Jun	2.5	Optimal	no	Low	yes	yes	bacia	2 dias	Bomba pedestral 44 L/m	18.0
NH_ZF_01_04	sandy clay	moderate	Cabbage	Repolho	15/Jun	2.5	Optimal	no	Low	yes	yes	bacia	2 dias	Bomba pedestral 44 L/m	5.0
NH_ZF_01_05	sandy clay	moderate	Tomato	Tomate	15/Jun	2.8	Optimal	no	Low	yes	yes	bacia	2 dias	Bomba pedestral 44 L/m	12.0

Annex 2 – Comparison weather data

Weather data as measured at the three stations in the project (Moatize, Bárúè, and Nhamatanda) is compared with data from the satellite data products GLDAS and CFSR. Both computed reference evapotranspiration using the Penman-Monteith method. Results of the comparison using data of the irrigation season (May – September) 2019 is displayed below indicating a reasonably good correlation of 0.70 and a slope close to the 1:1 line.

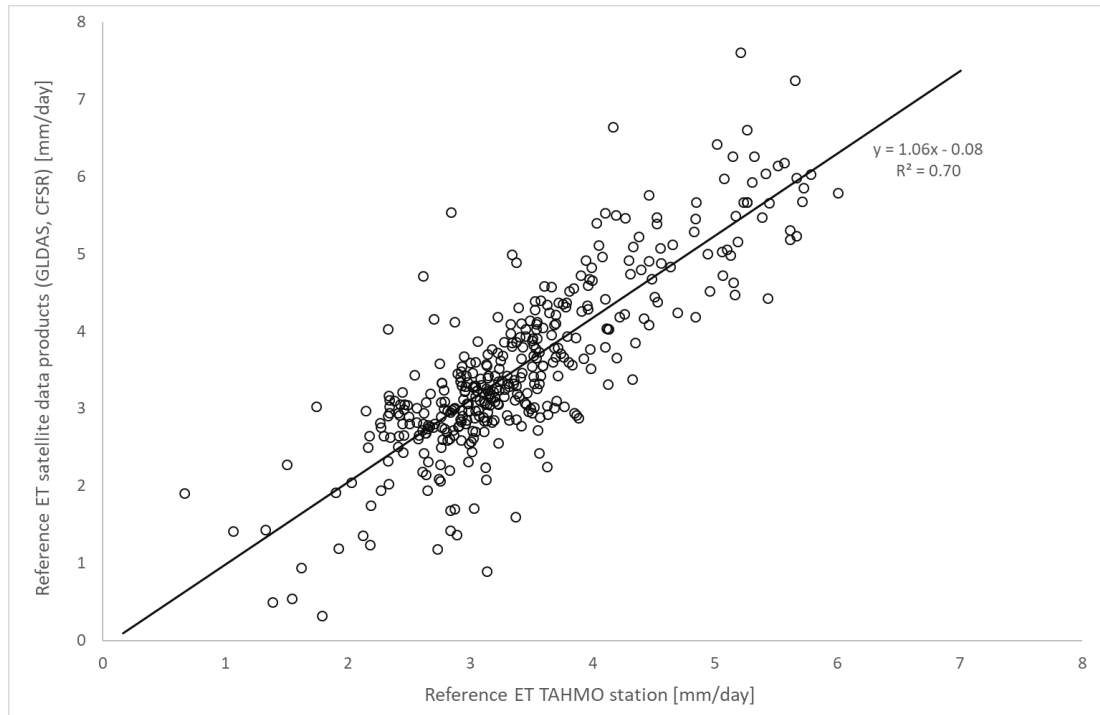


Figure 21 Comparison of reference ET as measured at the TAHMO stations of Bárúè, Moatize, and Nhamatanda, and the reference ET as calculated using satellite data products (GLDAS and CFSR)

Annex 3 – Additional basin results

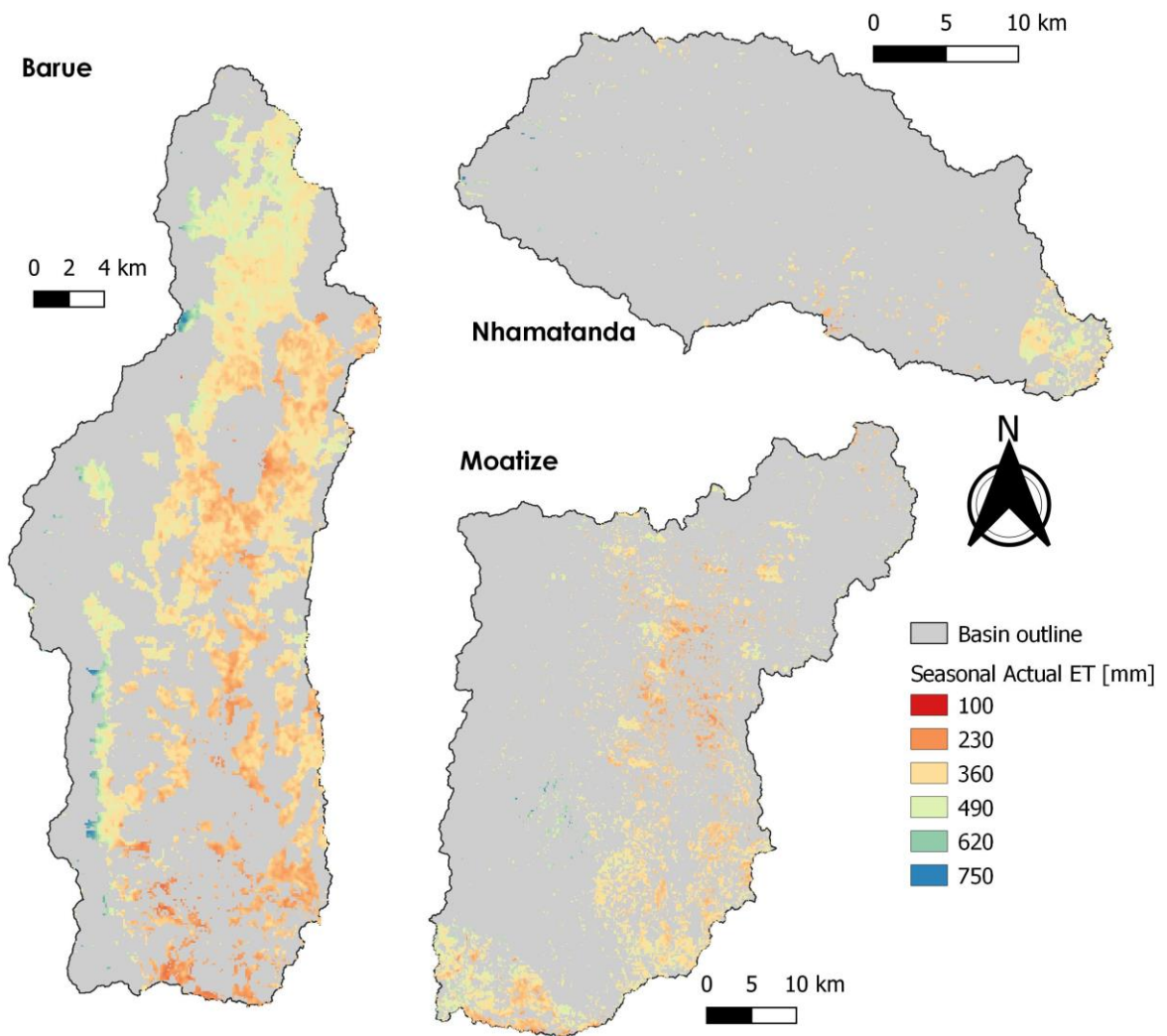


Figure 22 Seasonal actual evapotranspiration for the irrigation season from WaPOR data portal

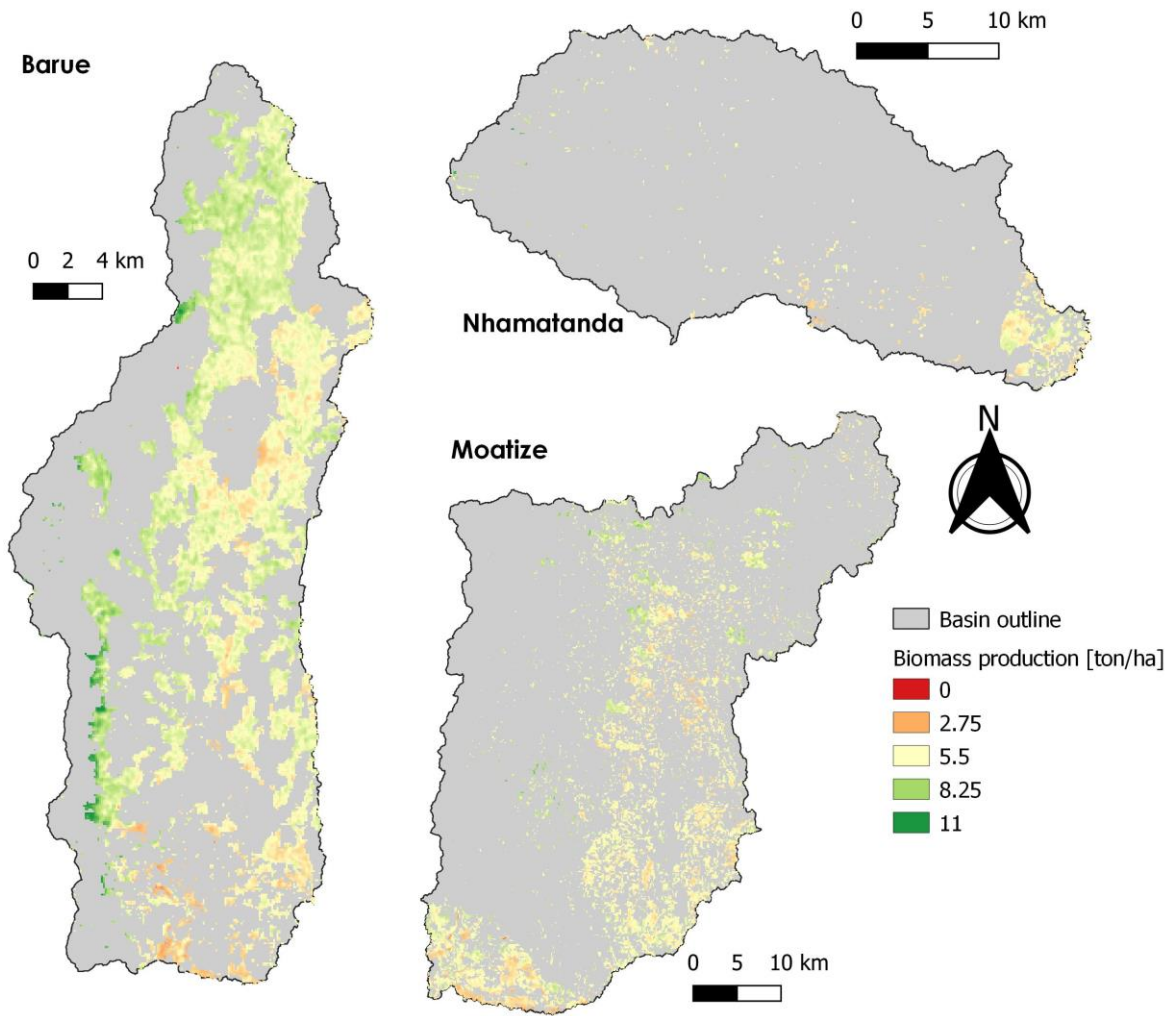


Figure 23 Biomass production for the irrigation season from the WaPOR data portal